Ultra-high tunable liquid crystal-plasmonic photonic crystal fiber polarization filter

Mohamed Farhat O. Hameed,[1,2] A. M. Heikal,[1,3] B. M. Younis,[1,3] Maher Abdelrazzak,[3] and S. S. A. Obayya[1,*]

[1]*Centre for Photonics and Smart Materials, Zewail City of Science and Technology, Cairo, Egypt*
[2]*Mathematics and Engineering Physics Department, Faculty of Engineering, Mansoura University, Mansoura, Egypt*
[3]*Electronics and Communications Engineering Department, Faculty of Engineering, Mansoura University, Mansoura, Egypt*
[*]*sobayya@zewailcity.edu.eg*

Abstract: A novel ultra-high tunable photonic crystal fiber (PCF) polarization filter is proposed and analyzed using finite element method. The suggested design has a central hole infiltrated with a nematic liquid crystal (NLC) that offers high tunability with temperature and external electric field. Moreover, the PCF is selectively filled with metal wires into cladding air holes. Results show that the resonance losses and wavelengths are different in x and y polarized directions depending on the rotation angle φ of the NLC. The reported filter of compact device length 0.5 *mm* can achieve 600 *dB / cm* resonance losses at φ = 90° for x-polarized mode at communication wavelength of 1300 *mm* with low losses of 0.00751 *dB / cm* for y-polarized mode. However, resonance losses of 157.71 *dB / cm* at φ = 0° can be achieved for y-polarized mode at the same wavelength with low losses of 0.092 *dB / cm* for x-polarized mode.

©2015 Optical Society of America

OCIS codes: (060.2310) Fiber optics; (060.5295) Photonic crystal fibers; (060.2340) Fiber optics components; (240.6680) Surface plasmons; (160.3710) Liquid crystals.

References and links

1. D. Noordegraaf, L. Scolari, J. Laegsgaard, T. Tanggaard Alkeskjold, G. Tartarini, E. Borelli, P. Bassi, J. Li, and S. T. Wu, "Avoided-crossing-based liquid-crystal photonic-bandgap notch filter," Opt. Lett. **33**(9), 986–988 (2008).
2. M. F. O. Hameed and S. S. A. Obayya, "Coupling characteristics of dual liquid crystal core soft glass photonic crystal fiber," IEEE J. Quantum Electron. **47**(10), 1283–1290 (2011).
3. A. M. Heikal, M. F. O. Hameed, and S. S. A. Obayya, "Improved trenched channel plasmonic waveguide," J. Lightwave Technol. **31**(13), 2184–2191 (2013).
4. B. Ortega, L. Dong, W. F. Liu, J. P. de Sandro, L. Reekie, S. I. Tsypina, V. N. Bagratashvili, and R. I. Laming, "High-performance optical fiber polarizers based on long-period gratings in birefringent optical fibers," IEEE Photon. Technol. Lett. **9**(10), 1370–1372 (1997).
5. Y. Wang, L. Xiao, D. N. Wang, and W. Jin, "In-fiber polarizer based on a long-period fiber grating written on photonic crystal fiber," Opt. Lett. **32**(9), 1035–1037 (2007).
6. Z. Yan, K. Zhou, and L. Zhang, "In-fiber linear polarizer based on UV-inscribed 45° tilted grating in polarization maintaining fiber," Opt. Lett. **37**(18), 3819–3821 (2012).
7. X. Zheng, Y. Liu, Z. Wang, T. Han, and B. Tai, "Tunable single polarization single-mode photonic crystal fiber based on liquid infiltrating," IEEE Photon. Technol. Lett. **23**(11), 709–711 (2011).
8. W. Qian, C. L. Zhao, Y. Wang, C. C. Chan, S. Liu, and W. Jin, "Partially liquid-filled hollow-core photonic crystal fiber polarizer," Opt. Lett. **36**(16), 3296–3298 (2011).
9. L. Scolari, T. Alkeskjold, J. Riishede, A. Bjarklev, D. Hermann, A. Anawati, M. Nielsen, and P. Bassi, "Continuously tunable devices based on electrical control of dual-frequency liquid crystal filled photonic bandgap fibers," Opt. Express **13**(19), 7483–7496 (2005).
10. W. Lei, T. T. Alkeskjold, and A. Bjarklev, "Compact design of an electrically tunable and rotatable polarizer based on a liquid crystal photonic bandgap fiber," IEEE Photon. Technol. Lett. **21**(21), 1633–1635 (2009).
11. M. A. Schmidt and P. St. J. Russell, "Long-range spiraling surface plasmon modes on metallic nanowires," Opt. Express **16**(18), 13617–13623 (2008).

#225167 - $15.00 USD Received 16 Oct 2014; revised 18 Dec 2014; accepted 29 Dec 2014; published 9 Mar 2015
(C) 2015 OSA

12. H. W. Lee, M. A. Schmidt, H. K. Tyagi, L. N. P. Sempere, and P. St. J. Russell, "Transmission properties of selectively gold-filled polarization-maintaining PCF," Conference on Lasers and Electro-Optics / Quantum Electronics and Laser Science Conference (CLEO/QELS), paper CFO3 (2008).
13. H. W. Lee, M. A. Schmidt, H. K. Tyagi, L. P. Sempere, and P. S. J. Russell, "Polarization-dependent coupling to plasmon modes on submicron gold wire in photonic crystal fiber," Appl. Phys. Lett. **93**(11), 111102 (2008).
14. X. Zhang, R. Wang, F. M. Cox, B. T. Kuhlmey, and M. C. J. Large, "Selective coating of holes in microstructured optical fiber and its application to in-fiber absorptive polarizers," Opt. Express **15**(24), 16270–16278 (2007).
15. H. K. Tyagi, H. W. Lee, P. Uebel, M. A. Schmidt, N. Joly, M. Scharrer, and P. St. J. Russell, "Plasmon resonances on gold nanowires directly drawn in a step-index fiber," Opt. Lett. **35**(15), 2573–2575 (2010).
16. S. S. A. Obayya, *Computational Photonics* (John Wiley & Sons, 2011).
17. A. Nagasaki, K. Saitoh, and M. Koshiba, "Polarization characteristics of photonic crystal fibers selectively filled with metal wires into cladding air holes," Opt. Express **19**(4), 3799–3808 (2011).
18. J. Xue, S. Li, Y. Xiao, W. Qin, X. Xin, and X. Zhu, "Polarization filter characters of the gold-coated and the liquid filled photonic crystal fiber based on surface plasmon resonance," Opt. Express **21**(11), 13733–13740 (2013).
19. M. W. Haakestad, T. T. Alkeskjold, M. Nielsen, L. Scolari, J. Riishede, H. E. Engan, and A. Bjarklev, "Electrically tunable photonic bandgap guidance in a liquid-crystal-filled photonic crystal fiber," IEEE Photon. Technol. Lett. **17**(4), 819–821 (2005).
20. S. Das, A. J. Dutta, N. Patwary, and M. S. Alam, "Characteristic analysis of polarization and dispersion properties of PANDA fiber using finite element methods," The AUST Journal of Science and Technology **3**(2), 3–8 (2013).
21. C. Kalnins, H. Ebendorff-Heidepriem, N. Spooner, and T. Monro, "Radiation dosimetry using optically stimulated luminescence in fluoride phosphate optical fibres," Opt. Mater. Express **2**(1), 62–70 (2012).
22. T. Alkeskjold, J. Lægsgaard, A. Bjarklev, D. Hermann, A. Anawati, J. Broeng, J. Li, and S. T. Wu, "All-optical modulation in dye-doped nematic liquid crystal photonic bandgap fibers," Opt. Express **12**(24), 5857–5871 (2004).
23. C. Hu and J. R. Whinnery, "Losses of a nematic liquid-crystal optical waveguide," J. Opt. Soc. Am. **64**(11), 1424–1432 (1974).
24. M. Green and S. J. Madden, "Low loss nematic liquid crystal cored fiber waveguides," Appl. Opt. **28**(24), 5202–5203 (1989).

1. Introduction

Photonic crystal fibers (PCFs) [1, 2] have attracted the interest of many researchers all over the world during the last years. PCFs are mainly composed of two dimensional triangular lattice of air holes rings along the whole length of the fiber. The electromagnetic light wave can be guided through PCFs in ways not previously possible or even imaginable. The guiding through solid core PCFs occurs by modified total internal reflection mechanism. However, the light wave can be confined through hollow core PCFs due to photonic bandgap guidance. PCFs have also unique properties such as endlessly single-mode operation, unusual chromatic dispersion, high birefringence, high or low nonlinearity……etc. In addition, the optical characteristics of PCFs can be improved by selectively filling the cladding air holes with different materials such as metals [1] or liquid crystals (LCs) [2].

'Plasmonics' is a new term in optics that refers to applications or phenomena in which surface plasmons (SPs) are involved. The surface plasmons polaritons (SPPs) are the interaction of surface electrons of metals with electromagnetic fields of incident light [3].The SPs may be of propagating or localized type. The difference between the behavior of surface electrons and those in the bulk metals has been known for a long time. However, scientists and engineers of several disciplines have recently turned their attention to these peculiarities and their applications. This is due to the technological advancements that have allowed fabrication and patterning of metallic structures in nanometer scale.

Optical fiber polarizing devices have a great importance in both fiber sensing systems and optical communication systems. There are two main techniques to build fiber-polarizing devices. In the first approach, grating on fiber is used. In this regard, fiber-grating-based polarizing devices have been presented such as high-performance optical fiber polarizers based on long-period gratings in birefringent PCFs [4, 5]. In addition, in-fiber linear polarizer based on UV-inscribed 45º tilted grating in polarization maintaining fiber has been introduced [6]. The fiber-grating-based polarizing devices have many advantages including

#225167 - $15.00 USD Received 16 Oct 2014; revised 18 Dec 2014; accepted 29 Dec 2014; published 9 Mar 2015
(C) 2015 OSA

compact structure, narrowband spectrum and low insertion loss. However, the other approach for realizing polarization-dependent devices is filling liquids [7, 8] or LCs into PCFs [1, 2]. This technique helps to construct devices, which are more easily tunable, controllable and can be flexibly designed than the other devices based on fiber gratings. At 2011, Zheng *et al*. proposed an adaptable single polarization single mode high birefringence PCF based on selectively filling cladding-air holes with liquid material [7].This structure achieved an adjustable sensitivity of 1.975 nm/ºC about three orders of magnitude higher than the polarizer based on long-period fiber grating [4]. In the same year, a fiber polarizer was constructed by filling some air holes of a hollow-core PCF partially with weak temperature dependent liquid [8]. In addition, some anisotropic liquids [9, 10] are used to design fiber-polarizing devices. In this regard, an electrically tunable and rotatable polarizer was designed by infiltrating LC into PCF [9, 10].

In metal-filled PCFs, surface plasmon modes are guided on metallic nanowires surface of circular cross-section embedded in a silica glass [11]. In this case, the light guided in the fiber-core can be coupled to SPPs if phase matching condition happens. The transmission in metal-filled PCFs depends strongly on the wavelength because the core guided light couples to leaky SPPs at certain wavelengths. By filling individual air holes with metal, one can get polarization-dependent transmission [11–13]. Lee *et al.* [13] have reported polarization dependent characteristics of polarization-maintaining PCFs with a gold nanowire and highly polarization and wavelength-dependent transmission. In addition, Zhang *et al*. [14] have presented selective silver coating in PCFs, in order to be applicable as absorptive polarizers. Moreover, Yagi *et al*. [15] have introduced step-index fibers with a gold wire in the fiber core region. However, these reported fibers do not have sufficient performance for polarizers. A sufficient method for realizing polarizers is to use both liquids or LCs and metals. This will give an easy and flexible way to design tunable and controllable devices.

In this paper, a novel design of single-core plasmonic liquid crystal PCF (PLC-PCF) filter is proposed and analyzed using full vectorial finite element method (FVFEM) [16] with minimum element size of $0.0008\,\mu m$. The PLC-PCF filter design has a metal wire at the central hole of the cladding region. In addition, a large hole in the core region is infiltrated with a nematic LC (NLC) of type $E7$. The effects of the structure geometrical parameters, temperature and rotation angle of the director of the NLC on the modal characteristics of the proposed design are investigated in detail. The analyzed parameters are effective index (n_{eff})and attenuation loss (α). It is evident from the simulation results that the designed filter has high tunability with external electric filed applied to the NLC infiltrated in the fiber core. In addition, the suggested filter of compact device length of $0.5\,mm$ can pass the y-polarized mode at $\varphi = 90º$ with high losses of $600\,dB/cm$ for the x-polarized mode at communication wavelength $\lambda = 1300\,nm$. However, the x-polarized mode can be obtained at the same wavelength at $\varphi = 0º$ with resonance losses of $157.71\,dB/cm$ for the y-polarized mode. Therefore, the suggested filter has high tunability due to the infiltration of the NLC material than those reported in the literature [17, 18]. The suggested filter has better polarization characteristics than that investigated by Nagasaki *et al.* [17]. The resonance strength of the PCF selectively filled with metal wires into cladding air holes is not strong enough and there are more than one resonance peak [17]. Additionally, the proposed PLC-PCF filter has stronger resonance strength than that presented by Xue *et al.* [18] at the same communication window. Further, the reported structure in [18] depends on using PCF with different hole diameters in the cladding region. Moreover, the suggested filter has high tunability due to the infiltration of NLC material.

#225167 - $15.00 USD Received 16 Oct 2014; revised 18 Dec 2014; accepted 29 Dec 2014; published 9 Mar 2015
(C) 2015 OSA

2. Design consideration

Figure 1 shows the proposed PLC-PCF filter. The suggested PCF has a fluorite crown of type FK51A as a background material and the cladding air holes of diameter $d_1 = 2\,\mu m$ are arranged in hexagonal shape with a lattice constant $\Lambda = 3.75\,\mu m$. In addition, a gold metal wire of diameter $d_c = 2\,\mu m$ is selectively filled in the cladding air holes. Moreover, a large hole of diameter $d_2 = 3.4\,\mu m$ infiltrated by NLC is inserted in the core region. The NLCs used in the proposed structure are anisotropic materials consisting of rod-like molecules, which are characterized by ordinary index n_o, and extraordinary index n_e. The relative permittivity tensor of the NLC [2] takes the following form:

$$\varepsilon_r = \begin{pmatrix} n_o^2 \sin^2\varphi + n_e^2 \cos^2\varphi & \left(n_e^2 - n_o^2\right)\sin\varphi\cos\varphi & 0 \\ \left(n_e^2 - n_o^2\right)\sin\varphi\cos\varphi & n_o^2 \cos^2\varphi + n_e^2 \sin^2\varphi & 0 \\ 0 & 0 & n_o^2 \end{pmatrix} \tag{1}$$

Where φ is the rotation angle of the director of the NLC. The proposed in plane alignment of the NLC can be exhibited under the influence of an appropriate homeotropic anchoring conditions [2]. The n_o and n_e of $E7$ material can be calculated using the following Cauchy models [2]

$$\begin{aligned} n_e &= A_e + \left(\frac{B_e}{\lambda^2}\right) + \left(\frac{C_e}{\lambda^4}\right) \\ n_o &= A_o + \left(\frac{B_o}{\lambda^2}\right) + \left(\frac{C_o}{\lambda^4}\right) \end{aligned} \tag{2}$$

where $A_e, B_e, C_e, A_o,$ B_o and C_o are the coefficients of the Cauchy model. The Cauchy coefficients at $T = 25$ºC are $A_e = 1.6933$, $B_e = 0.0078\,\mu m^2$, $C_e = 0.0028\,\mu m^4$, $A_o = 1.4994$, $B_o = 0.007\,\mu m^2$, and $C_o = 0.0004\,\mu m^4$.

The NLC director's orientation can be controlled by applying an external static electric field as described by Haakestad *et al.* [19]. The spacing between the electrodes and the PCF can be controlled using two silica rods. As a result, the NLC core will be affected by uniform external electric filed line distribution. However, the nonuniform electric field lines at the edges of the electrodes will be far away from the NLC core. Therefore, the director of the NLC will have good alignment with constant rotation angle φ. It should also be noted that sets of electrodes can be used as described by Lei *et al.* [10] to control the alignment of the NLC molecules.

The Sellmeier equation of the FK51A material [20] is given by:

$$n^2(\lambda) = 1 + \frac{A_1\lambda^2}{\lambda^2 - B_1} + \frac{A_2\lambda^2}{\lambda^2 - B_2} + \frac{A_3\lambda^2}{\lambda^2 - B_3} \tag{3}$$

where $n(\lambda)$ is the wavelength dependent refractive index of the FK51A, $A_1 = 0.971247817$, $A_2 = 0.2169014$, $A_3 = 0.9046517$, $B_1 = 0.00472302\,\mu m^2$, $B_2 = 0.01535756\,\mu m^2$ and $B_3 = 168.68133\,\mu m^2$. The proposed polarization PCF filter depends on high birefringent NLC core and a metal wire filled in one of the cladding air holes. The NLC has two principal

#225167 - $15.00 USD Received 16 Oct 2014; revised 18 Dec 2014; accepted 29 Dec 2014; published 9 Mar 2015
(C) 2015 OSA

refractive indices, n_e and n_o for the extraordinary and ordinary rays, respectively. The coupling between the two orthogonal polarized core modes (x and y-polarized modes) and the plasmonic modes can be controlled using the birefringence of the NLC material. The energy coupling efficiency between the plasmonic modes and one of orthogonal polarization core mode (the mode to be suppressed) can be enhanced by decreasing the difference between the ordinary refractive index of NLC core ($n_o = 1.5037 at \lambda = 1.3 \mu m$) and that of the background material. Through the reduction of the index difference, the coupling between the lossy-in-nature plasmonic modes and polarization mode (to be suppressed) can be highly improved, consequently, the core mode (to be suppressed) starts to lese power very quickly leading to a more compact mode filter design. Hence the choice of the FK51A glass ($n = 1.4777 at \lambda = 1.3 \mu m$) is justified to give us a better control over the offered design in terms of compactness. Additionally, optical fiber based on FK51A glass can be now fabricated using the well-known stack and draw technology [21]. Therefore, the suggested FK51APCF can be fabricated using the stack and draw technique [21].

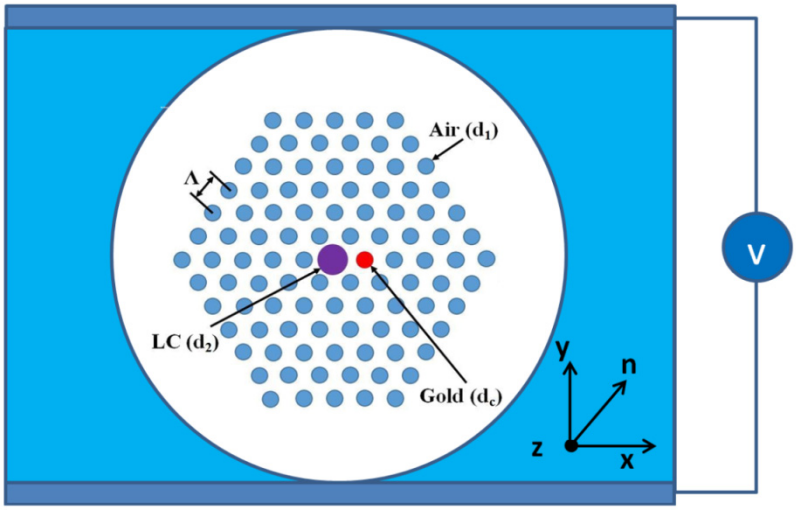

Fig. 1. Cross section of the PLC-PCF filter filled with a metal wire and sandwiched between two electrodes.

The relative permittivity of gold in the visible and near IR-region can be expressed as [3]:

$$\varepsilon_{Au}(\omega) = \varepsilon_{\infty} - \frac{\omega_p^2}{\omega(\omega + i\omega_\tau)} \tag{4}$$

where $\varepsilon_{\infty} = 9.75$, $\omega_p = 1.36 \times 10^{16} rad/s$ and $\omega_\tau = 1.45 \times 10^{14} rad/s$.

It is worth to know that the effective index of the NLC material at any wavelength through the range is greater than that of the background material at the same wavelength. Therefore, the propagation through the NLC core occurs by modified total internal reflection. In addition, there are two main fundamental core modes that will be guided through the fiber core, x-polarized and y-polarized modes. One of these two fundamental modes will couple with the surface of the metal wire while the other will propagate through the fiber without any coupling. The coupling operation depends on the molecule directions of the NLC material which will determine the coupled core mode to the metal surface. The n_e and n_o of the E7 material are temperature dependent. Consequently, the reported filter has high tunability with

#225167 - $15.00 USD Received 16 Oct 2014; revised 18 Dec 2014; accepted 29 Dec 2014; published 9 Mar 2015
(C) 2015 OSA

temperature. In addition, the performance of the reported filter can be tuned using the structure geometrical parameters.

3. Simulation results

First, numerical investigation of the electric field distribution across the suggested design has been done. In order to study the strength and the distribution of the electric field through the proposed structure, the equation $\nabla \cdot \mathrm{D} = \varepsilon(\mathrm{x},\mathrm{y})\,\mathrm{E} = 0$ has been solved using finite element method where D is the dielectric displacement, E is the electric field and $\varepsilon(\mathrm{x},\mathrm{y})$ is the dielectric permittivity profile. In the numerical simulation, to reduce the simulation time, the width of the electrodes was taken as 12 times the hole-pitch of the proposed structure as shown in Fig. 2. This was enough to avoid electrode edge effects that could influence the field within the fiber. The polarization extinction ratio for liquid crystal is continuously tuned when the driving voltage V is above the Fredericks threshold [10]. Therefore, in this simulation $\mathrm{V}_{rms} = 40\,\mathrm{V}$ is applied. Figure 2 shows the contour lines of the electric potential (V) (horizontal gray solid lines) and normalized arrow surface of E-field distribution (vertical red arrows) across the proposed structure. It is revealed from Fig. 2 that the E-field distribution is still uniform inside the NLC core even in the presence of metal wires. Moreover, although, expected nonuniform around the metal wire, the electric field lines are clearly uniform inside the NLC core as shown in Fig. 2. As a result, an accurate director angle $\varphi = 0^{\circ}$ or $\varphi = 90^{\circ}$ can be obtained using the two electrodes arrangement.

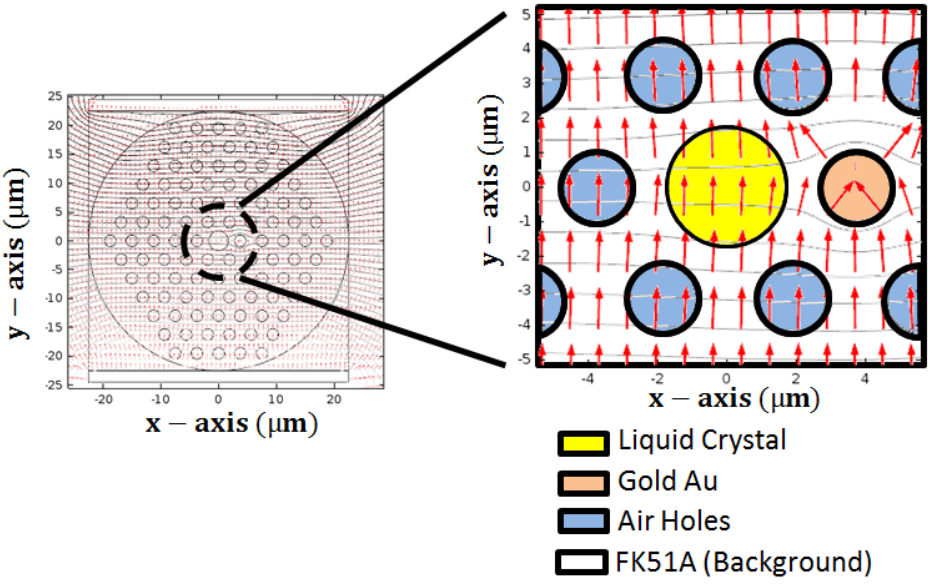

Fig. 2. Contour lines of electric potential (V) (horizontal gray solid lines) and normalized arrow surface of E-field distribution (vertical red arrows) across the proposed structure

The polarization characteristics of the two fundamental polarized mode of the suggested filter are then studied and analyzed. Figure 3 shows the wavelength dependence of the effective indices of the different modes in the PCF (x-polarized core mode, y-polarized core mode, SP^0, SP^1, SP^2, SP^3 and SP^4 modes) at $T = 25\,°\boldsymbol{C}$ and $\varphi = 90^{o}$. At $\varphi = 90^{o}$, the director of the NLC is normal to E_x and is parallel to E_y and the dielectric permittivity tensor ε_r of the $E7$ material has the diagonal form $\left[n_o^2, n_e^2, n_o^2\right]$. In this case, ε_{xx} is smaller

#225167 - $15.00 USD Received 16 Oct 2014; revised 18 Dec 2014; accepted 29 Dec 2014; published 9 Mar 2015
(C) 2015 OSA

than ε_{yy} therefore, the effective index of the x-polarized mode is smaller than that of the y-polarized mode as shown in Fig. 3. It is also revealed from Fig. 3(b) that the effective index of the y-polarized mode is greater than the SP modes, therefore no coupling occurs.

It is also evident from Fig. 3 that the x-polarized mode is only coupled to the higher order surface plasmon modes (SP^2, SP^3 *and* SP^4) due to phase matching between them at resonance wavelengths of $1162\,nm$, $920\,nm$ and $785\,nm$, respectively. In this case, the effective indices for the two coupled modes are equal at their resonance wavelength. However the y-polarized core mode makes no coupling because of the absence of phase matching with the surface plasmon modes. Therefore, the polarization filter behavior is very obvious as the y-polarized core mode will pass through the fiber with no change, while the x-polarized core mode will not pass due to the coupling with the surface plasmon modes.

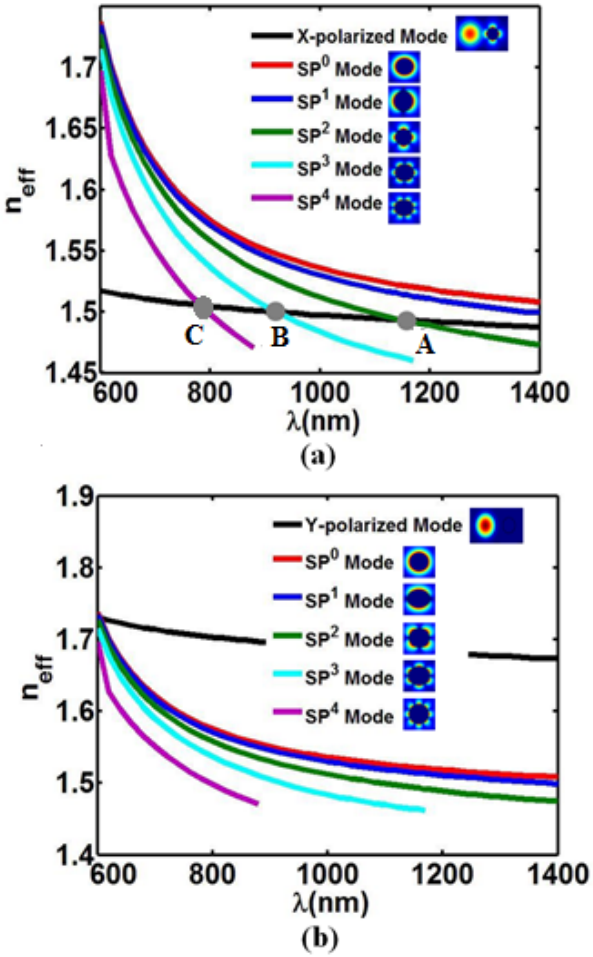

Fig. 3. Wavelength dependence of effective indices of (a) x-polarized core mode and surface plasmon (SP^0 , SP^1 , SP^2 , SP^3 and SP^4) modes. (b) y-polarized core mode and surface plasmon (SP^0 , SP^1 , SP^2 , SP^3 and SP^4) modes. Points A, B and C are the intersection points of the x-polarized core mode dispersion curve with the SP^2 , SP^3 and SP^4 modes dispersion curves, respectively, while $T = 25°C$ and $\varphi = 90^o$.

#225167 - $15.00 USD Received 16 Oct 2014; revised 18 Dec 2014; accepted 29 Dec 2014; published 9 Mar 2015
(C) 2015 OSA

Figure 4 shows the calculated attenuation loss of the two fundamental core modes. It is revealed from Fig. 4 that there are three peaks at $\lambda = 1162$ *nm*,920 *nm* and 780 *nm* due to the coupling of the x-polarized core mode with the SP^2, SP^3 and SP^4 modes, respectively. The three coupling points with SP^2, SP^3 and SP^4 modes are indicated in Fig. 4 as points A, B and C, respectively. On the other hand, the attenuation curve of the y-polarized mode is very low for the entire wavelength range, which reveals the behavior of the polarization filter.

In order to prove our results, field plots of the two polarized core modes at different wavelengths 900, 116 and 1300 *nm* are shown in Fig. 5. As may be seen in Fig. 5, there is a strong coupling between the x-polarized core mode and SP^2 mode at resonance wavelength ($\lambda_r = 1162\,nm$). However, at $\lambda = 900$ *nm* and $\lambda = 900$ *nm* most of the electric field is coupled to the fiber core. It is also clear from Fig. 5 that the y-polarized mode is well confined in the fiber core through the entire wavelength range with no *SP* modes coupling.

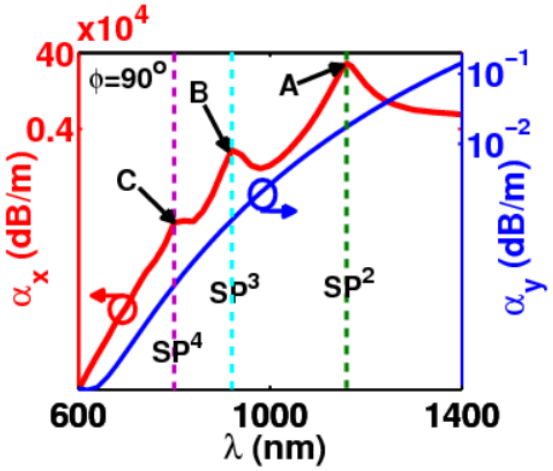

Fig. 4. Loss spectrum (in log scale) for the x-polarized and y-polarized core modes at $T = 25°C$, and $\varphi = 90^o$. Points A, B and C are the equivalent points to the resonance wavelengths shown in Fig. 3 (a).

One of the most effective parameters on the behavior of the suggested filter is the rotation angle (φ) of the NLC material which can be easily controlled by changing the applied electric field. Figure 6 shows the attenuation loss behavior of the two core modes, x-polarized and y-polarized modes at $\varphi = 0^o$ and $\varphi = 90^o$. It is clear from Fig. 6 that the filter operation is inverted with the rotation angle change from $\varphi = 90^o$ to $\varphi = 0^o$. At $\varphi = 0^o$, the y-polarized mode couples with the *SP* modes while the x-polarized mode makes no coupling as shown in Fig. 6. It should be noted that the x-polarized mode is coupled strongly at $\varphi = 90^o$ with a loss peak of $\alpha_x = 28500\,dB/m$, which is larger than the other peak of the coupled y-polarized mode at $\varphi = 0^o$ with $\alpha_y = 8500\,dB/m$. This is due to the position of the metal wire, which is aligned horizontally relating to the core region.

#225167 - $15.00 USD Received 16 Oct 2014; revised 18 Dec 2014; accepted 29 Dec 2014; published 9 Mar 2015
(C) 2015 OSA

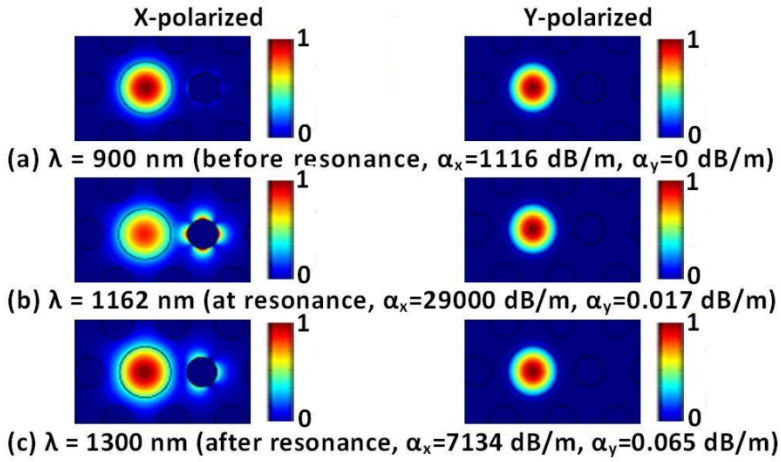
X-polarized
Y-polarized
1
0
(a) λ = 900 nm (before resonance, αx=1116 dB/m, αy=0 dB/m)
(b) λ = 1162 nm (at resonance, αx=29000 dB/m, αy=0.017 dB/m)
(c) λ = 1300 nm (after resonance, αx=7134 dB/m, αy=0.065 dB/m)

Fig. 5. Field plots of x and y polarized core modes at different wavelengths (a) before resonance at $900\,nm$, (b) at resonance at $\lambda = 1162\,nm$ and (c) after resonance at $\lambda = 1300\,nm$.

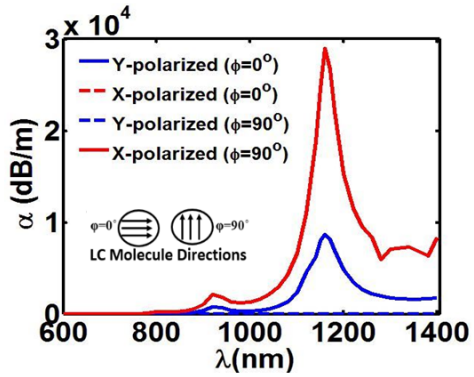

Fig. 6. Variation of the attenuation losses of the two fundamental polarized modes at $\varphi = 90^o$ and $\varphi = 0^o$ while the temperature is fixed at $T = 25°C$. The molecules directions related to the rotation angle are shown in the inset figure.

At $\varphi = 0^o$, the electric permittivity tensor ε_r has the diagonal form of $\left[n_e^2, n_o^2, n_o^2\right]$. Therefore, ε_{xx} is greater than ε_{yy} and hence the x-polarized mode effective index is greater than those of the SP modes. Hence there is no coupling occurs with the x-polarized mode at $\varphi = 0^o$ .It is also evident from Fig. 6 that the rotation angle has no effect on the resonance wavelength at which the two polarized core modes are coupled to the SP modes at $\varphi = 0^o$ and $\varphi = 90^o$.

#225167 - $15.00 USD Received 16 Oct 2014; revised 18 Dec 2014; accepted 29 Dec 2014; published 9 Mar 2015
(C) 2015 OSA

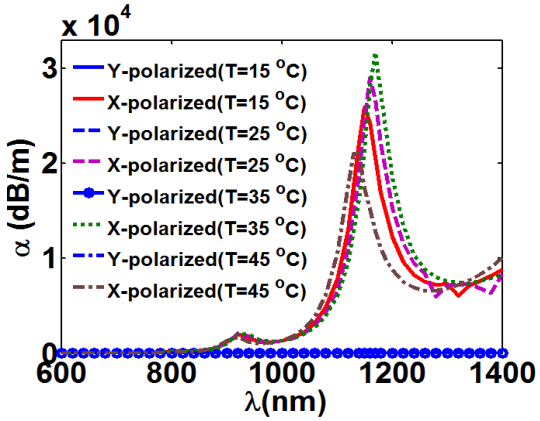

Fig. 7. Variation of attenuation losses of the two fundamental polarized core modes at different temperatures while the rotation angle φ is fixed at 90^o

The effect of the temperature on the performance of the proposed filter is also investigated. Figure 7 shows the effect of variation of temperature on the filter behavior and resonance wavelength at $\varphi = 0^o$. It is revealed from Fig. 7 that the resonance wavelength of the coupled core-guided mode has a tunable behavior with the temperature. In this study, four different cases have been reported and discussed at $T = 15°\boldsymbol{C}$, $T = 25°\boldsymbol{C}$, $T = 35°\boldsymbol{C}$ and $T = 45°\boldsymbol{C}$ .The resonance wavelengths are found to be 1150, 1160, 1170 and 1140 *nm*, respectively. From these results, we can conclude that a $10°\boldsymbol{C}$ change in temperature gives a shift of 10 *nm* in resonance wavelength (λ_r). Therefore, the proposed polarization filter has a tunable sensitivity of about $1nm/°C$.

The polarization characteristics of the designed filter can be altered by changing the geometrical parameters of the PCF. In this part, the impacts of the cladding air holes diameter (d_1), metal diameter (d_c) and NLC central hole diameter (d_2) are analyzed and investigated. Figure 8 shows the variation of the two fundamental core-guided modes attenuation losses at different cladding air holes diameter (d_1). It is evident from Fig. 8 that the cladding air holes diameter has no effect on the resonance wavelength of the x-polarized mode. This is due to the well confinement of the mode field through the core region. It is worth noting that the y-polarized mode has approximately no losses through the whole spectrum.

#225167 - $15.00 USD Received 16 Oct 2014; revised 18 Dec 2014; accepted 29 Dec 2014; published 9 Mar 2015
(C) 2015 OSA

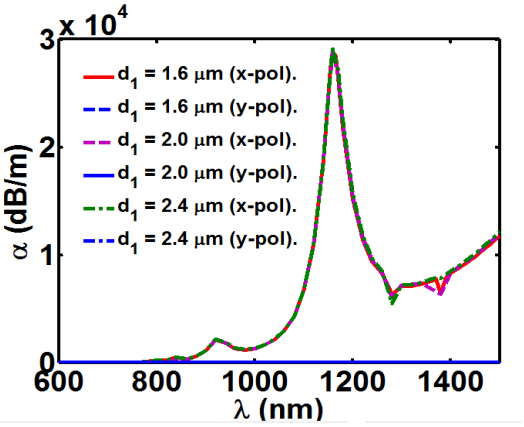

Fig. 8. Variation of the wavelength dependent attenuation losses of the two fundamental core modes (x-polarized and y-polarized mode) at different air hole diameters (d_2), 1.6 μm, 2 μm and 2.4 μm while $d_c = 2\,\mu m$, $d_2 = 3.4\,\mu m$, $T = 25°C$, and $\varphi = 90^o$.

It is well known that surface plasmon waves are extremely sensitive to the metal thickness. Figure 9 shows the variation of the attenuation loss of the two polarized modes as a function of the metal wire diameter (d_c) while all other PCF parameters are fixed to their original values. It is clear from Fig. 9 that the resonance wavelength increases as the metal wire diameter increases and the loss strength is significantly affected by changing the metal wire diameter. Therefore, one needs to be careful while choosing the metal wire diameter so that the desired effects could be achieved. It should be noted that at $d_c = 2.62\,\mu m$, the resonance wavelength is approximately equal to 1300 nm with resonance losses of $60000\,dB/m$ and $0.751\,dB/m$ at $\varphi = 90^o$ for x and y polarized modes, respectively. However, resonance losses of $15771\,dB/m$ at $\varphi = 0^o$ can be achieved for y-polarized mode at the same wavelength with 9.2 dB/m losses for x-polarized mode. It is well known that wavelength of 1300 nm lies in the second communication window of optical fibers $(1250-1350)nm$. For a filter design, it is required to achieve compact device length with high losses for one polarized mode while very low losses for the other polarized mode. Therefore, in order to optimally design the filter, it is required to achieve total leakage losses for the y-polarized mode $<0.1dB$ while the total leakage losses for the suppressed x polarized mode $>30dB$. It is found that these requirements can be achieved with compact device length of $0.5\,mm$ at $\varphi = 90^o$.

However, at $\varphi = 0^o$ compact device length of 1.9 nm will be needed to pass the x polarized only. Therefore, a suitable electrodes size can be chosen to cover the PCF length to keep the same refractive indices in the NLC core. It should also be noted that similar to any other fiber types, bending with small radii of curvature causes radiation losses. However, in the suggested design and thanks to the excellent confinement of light, the proposed fiber is expected to be subject to fallen radiation losses of bent. Additionally, the compact length can avoid the bending of the suggested filter.

#225167 - $15.00 USD Received 16 Oct 2014; revised 18 Dec 2014; accepted 29 Dec 2014; published 9 Mar 2015
(C) 2015 OSA

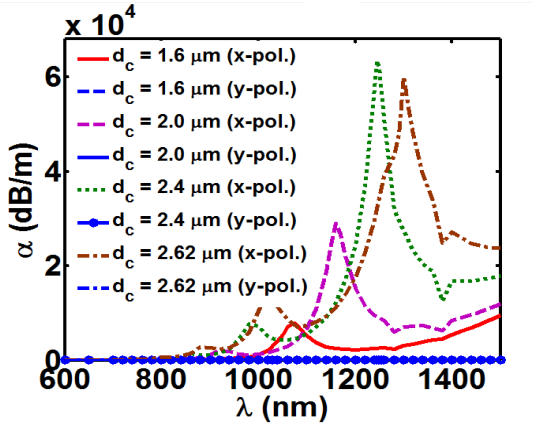

Fig. 9. Variation of attenuation losses of the two fundamental core modes (x-polarized and y-polarized mode) with the metal wire diameter (d_c)while d_1, d_2, T, and φ are taken as $2\mu m$, $3.4\mu m$, $25°C$ and $90°$, respectively.

Figure 10 shows the effect of variation of the attenuation loss of the two fundamental core modes (x-polarized and y-polarized mode) with the diameter (d_2) of the NLC infiltrated hole in the fiber core. It is evident from Fig. 10 that the diameter d_2 has a slight effect on the resonance wavelength. As d_2 increases from $3\mu m$ to $3.8\mu m$, the resonance wavelength decreases from 1185 *nm* to 1145 *nm*.

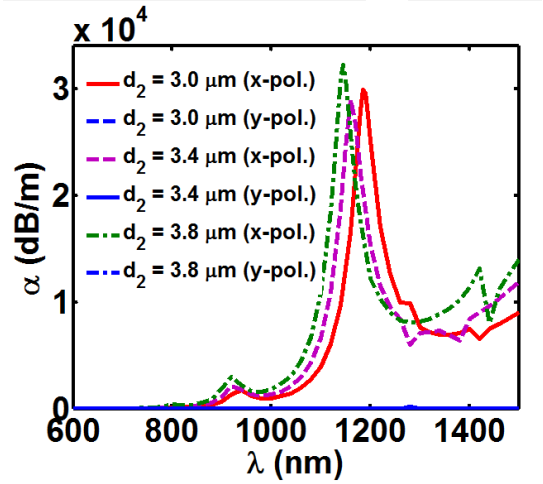

Fig. 10. Variation of attenuation losses of the two fundamental core modes (x-polarized and y-polarized mode) with the NLC central hole diameter (d_2) while d_1, d_2, T, and φ are taken as $2\mu m$, $2\mu m$, $25°C$ and $90°$, respectively.

A study on the effect of number of metal wires surrounding the NLC core is also investigated and analyzed. Figure 11 shows the variation of the wavelength dependent attenuation losses of the x-polarized core mode of the PLC-PCF with one and two metal wires. It is revealed from Fig. 11 that using metal wires on the two sides of the NLC core will enhance strongly the filter behavior. The attenuation loss of the PLC-PCF with two metal wires ($\alpha_x = 75000\,dB/m$) at the resonance wavelength will be 3-times larger than that with

#225167 - $15.00 USD Received 16 Oct 2014; revised 18 Dec 2014; accepted 29 Dec 2014; published 9 Mar 2015
(C) 2015 OSA

only one metal wire ($\alpha_x = 28500 dB/m$).It is also clear from Fig. 11 that the two cases have the same resonance wavelength. However, the use of second metal wire results in more sharp attenuation curve. Therefore, it is expected that increasing the number of metal wires around the NLC core will strongly enhance the filter operation.

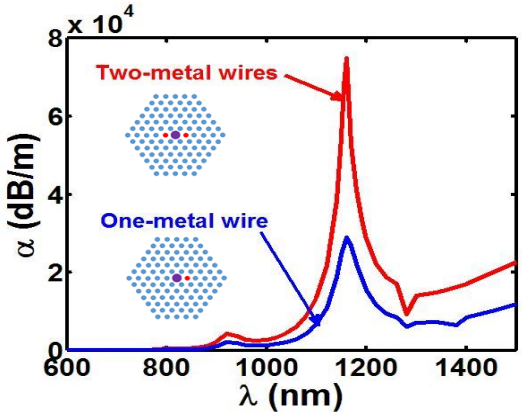

Fig. 11. Variation of the attenuation losses of the x-polarized core mode of the PLC-PCF with one and two metal wires with the wavelength.

It should be noted that the absorption and scattering losses of the NLC are much larger than that of background materials such as silica, Pyrex and FK51A [22]. Therefore, the background material loss can be ignored. In addition, the scattering losses of the bulk NLC of around 15 to 40 dB/cm reported by Hu and Whinnery [23] are much greater than its absorption losses at visible and near-infrared wavelengths. However, Green and Madden [24] show that the scattering loss of NLCs can be decreased to 1 to 3 *dB/cm* by infiltrating the LC into small capillaries with inner diameters of 2 to 8 μm . In this study [24], conventional Pyrex fibers with refractive index of 1.470 and core diameter of 4 μm was infiltrated by NLC whose director was aligned along the fiber axis. Laser light of wavelength 633 *nm* was focused on the fiber end and the scattered light out of the fiber normal to the propagation direction was observed. In this case, an average loss of $3.25 dB/cm$ was obtained. The scattering losses of silica fiber infiltrated by NLC have been also investigated [24]. Scattering losses of 1.5 to $2.4 dB/cm$ have been obtained along fiber length of $30 cm$. Therefore, the scattering losses in small core fibers are fewer than $20 dB/cm$ obtained after propagation in a slab waveguide or in a large diameter LC cored fiber [23]. Moreover, the scattering loss of the LC is dependent on the filling technique. In this regard, the infiltration of the LC using capillary forces has lower losses than when using high-pressure [24].

In this paper, central hole of diameter $d_2 = 3.4 \mu m$ is infiltrated by the NLC where the light is propagating through the NLC core in a fashion way similar to [24]. Moreover, the suggested filter has a compact length of $0.5 mm$. Further, a fluorite crown of type FK51A of refractive index of 1.477 is used as a background material which has a refractive index value very close to Pyrex fibers with refractive index of 1.470 [24]. Therefore, it is believed that the scattering losses will be less than 1.5 to $2.4 dB/cm$ [24] giving rise to a low scattering losses of 0.075 to $0.2 dB$ for our device of compact length of $0.5 mm$. However, for longer device where scattering losses can be an issue, an alignment layer can be used at the edges to help align the molecules near the edges so the scattering losses can be minimized.

5. Conclusion

A high tunable polarization filter, with tunable sensitivity of about $1 nm/°C$, based on PLC-PCF has been reported and analyzed. The numerical results demonstrate that the proposed

#225167 - $15.00 USD Received 16 Oct 2014; revised 18 Dec 2014; accepted 29 Dec 2014; published 9 Mar 2015
(C) 2015 OSA

filter has high tunability with the temperature and external electric field. In addition, the polarizer behavior can be inverted by changing the rotation angle of the NLC from $\varphi = 90^o$ to $\varphi = 0^o$ .Moreover, the performance of the suggested filter can be enhanced by increasing the number of metal nanowires used.

#225167 - $15.00 USD Received 16 Oct 2014; revised 18 Dec 2014; accepted 29 Dec 2014; published 9 Mar 2015
(C) 2015 OSA